Journal of Sound and Vibration (2001) **247**(4), 673–681
doi:10.1006/jsvi.2001.3779, available online at http://www.idealibrary.com on IDEAL®

SPECIMEN DESIGN FOR FATIGUE TESTING AT VERY HIGH FREQUENCIES

T. E. MATIKAS

Greek Atomic Energy Commission, P.O. Box 60092, 15310 *Agia Paraskevi Attikis, Athens Greece*

(*Received* 14 *August* 2000, *and in final form* 19 *April* 2001)

Components in rotational machinery such as turbine blades used in military aircraft engines are subjected to low-amplitude, high-frequency loads in the kHz range. Under high cycle fatigue (HCF), the initiation state of a crack consumes most of the life of the component. Vibratory stresses may therefore result in unexpected failures of the material. Hence, there is a need for HCF studies to address HCF-related failures of turbine engines and to develop a life prediction methodology. Ultrasonic fatigue provides accelerated HCF testing enabling the simulation of realistic loading conditions for testing materials used in structural components subjected to vibratory stresses. Specimen design is critical for optimum ultrasonic fatigue testing. The objective of this study is therefore to develop analytical modelling necessary for the design of test coupons to be fatigue tested at ultrasonic frequencies.

1. INTRODUCTION

Fatigue testing at ultrasonic frequencies was pioneered in the 1950s [1, 2]. Several researchers addressed the problem of designing resonant vibrators for a variety of applications [3–5], which include ultrasonic cleaning, welding, atomization of liquids, and mechanical testing of materials. The same principle is applied to all these applications. A transducer is used to convert an output voltage to a mechanical vibration. Different types of transducers, such as piezoelectric, piezomagnetic and electrodynamic, have been used in various configurations to provide ultrasonic loads [2, 6]. In the case of fatigue testing, the ultrasonic vibrating source induces compressional elastic waves to a specimen. For the test coupon to resonate at ultrasonic frequencies, the specimen length must be such that a standing displacement wave is formed along its length. The displacement wave in turn causes a strain wave that loads the specimen. A convenient range of operation of an apparatus used in ultrasonic fatigue testing in 10–40 kHz. There are advantages in using this frequency range in ultrasonic fatigue. First, frequencies greater than 18 kHz are above the audible range for humans. A second advantage in using this frequency range is the size of associated specimens and components. Since the resonant length of the specimen is inversely proportional to the frequency, there is a finite limit on the upper testing frequency that can be used. The 10–40 kHz range coincides with a specimen resonance length approximately 5–15 cm for most metals, thereby making this range attractive. Recently, a 20 kHz ultrasonic fatigue cell has been developed [7] that can be integrated to a servo-hydraulic loading frame enabling the superposition of low-frequency, high-amplitude stresses to the ultrasonic stresses.

The objective of this work is the optimization of the design of fatigue samples to be tested at ultrasonic frequencies. The analysis of specimen geometry presented in this paper

0022-460X/01/440673 + 09 $35.00/0

includes theoretical calculations of (a) the resonance length of the specimens, and (b) the strain and displacement along the length of specimens with different geometries and for various resonant frequencies.

2. MODELLING THE VIBRATION OF THE SPECIMEN

The speed of sound, c, for a compressional wave in a solid medium is dependent on material properties and the geometry of the specimen. In the case of an ultrasonic fatigue specimen, the wavelength, $\lambda = c/f$, where f denotes frequency, is much larger than the width of the specimen. Under these circumstances, it can be assumed that the normal stress is one dimensional in nature (along the axis of the specimen), with no stress in the lateral dimension. The speed of sound is then called "bar velocity" given by

$$c = \sqrt{\frac{E}{\rho}}, \tag{1}$$

where E is the Young's modulus and ρ is the density of the material.

In response to an excitation voltage, the piezoelectric transducer produces a displacement wave, which is transferred to the specimen. Since the excitation voltage is sinusoidal with a given frequency, f, the displacement wave produced by the transducer will also be sinusoidal with the same frequency. Assuming that the material is a solid, elastically linear medium, the displacements at any two points in the resonating body will be proportional to each other for any given time. Therefore, the material will resonate in a single mode and there will be a position on the solid body where the strain will be maximum, and a position where the displacement will be maximum.

For a cylindrical specimen the displacement wave $u(x, t)$ is defined by

$$u(x, t) = B\cos\left(\frac{2\pi f}{c}x\right)e^{i(2\pi f)t} = u(x)\,e^{i(2\pi f)t}. \tag{2}$$

Since the displacement in the cylinder is not uniform, the cylinder also undergoes a strain, $\varepsilon(x, t)$, which is defined by

$$\varepsilon(x, t) = \frac{\partial u(x, t)}{\partial x} = -B\frac{2\pi f}{c}\sin\left(\frac{2\pi f}{c}x\right)e^{i(2\pi f)t} \tag{3}$$

and the stress is

$$\sigma(x, t) = E\,\varepsilon(x, t). \tag{4}$$

Since the maximum strain occurs at $(2\pi f/c)x = \pi/2$, or $x = \lambda/4$, the specimen is designed with an overall length, L, equal to one-half-wavelength, so that the center of the specimen is the point of maximum strain (which corresponds to a node point for the displacement wave). Therefore, the resonance length of a cylindrical specimen is given by

$$L = \frac{1}{2f}\sqrt{\frac{E}{\rho}}. \tag{5}$$

Altering the cross-sectional area of the specimen serves as a means by which the amplitude of the stress and the strain at the center of the specimen is increased, when excited with displacement amplitude at the end of the sample. For that reason, a dog-bone-shaped specimen is preferred over the simple cylindrical specimen. With a dog-bone-shaped specimen, the magnitude of the displacement wave (and hence the strain wave which is produced) is amplified for a given input. The magnification factor is defined as the ratio of the strain at the longitudinal center of a dog-bone-shaped specimen to that at the center of a cylindrical specimen. The non-constant cross-section of the specimen also complicates the analysis for determining the resonant length.

In order to describe the vibration of the specimen in a purely longitudinal mode one can start with the equation of motion,

$$\rho A(x) \frac{\partial^2 u(x,t)}{\partial t^2} = \frac{\partial F(x,t)}{\partial x}, \tag{6}$$

where $A(x)$ is the cross-sectional area, and F the force.

In the elastic range,

$$F(x,t) = -E A(x) \frac{\partial u(x,t)}{\partial x}. \tag{7}$$

Therefore, equation (6) can be written as follows:

$$\frac{\rho}{E} \frac{\partial^2 u(x,t)}{\partial t^2} + \frac{1}{A(x)} \frac{\partial u(x,t)}{\partial x} \frac{\partial A(x)}{\partial x} + \frac{\partial^2 u(x,t)}{\partial x^2} = 0. \tag{8}$$

Introducing expression (2) for the displacement into equation (8) leads to a differential equation, which describes the spatial dependence of one-dimensional wave in a continuum.

$$\frac{\mathrm{d}^2 u(x)}{\mathrm{d}x^2} + G(x) \frac{\mathrm{d}u(x)}{\mathrm{d}x} + k^2 u(x) = 0, \tag{9}$$

where the non-constant coefficient $G(x)$ is a function defining the specimen geometry and is given by

$$G(x) = \frac{\mathrm{d}A(x)}{\mathrm{d}x} \frac{1}{A(x)} \tag{10}$$

and $k = 2\pi f/c$.

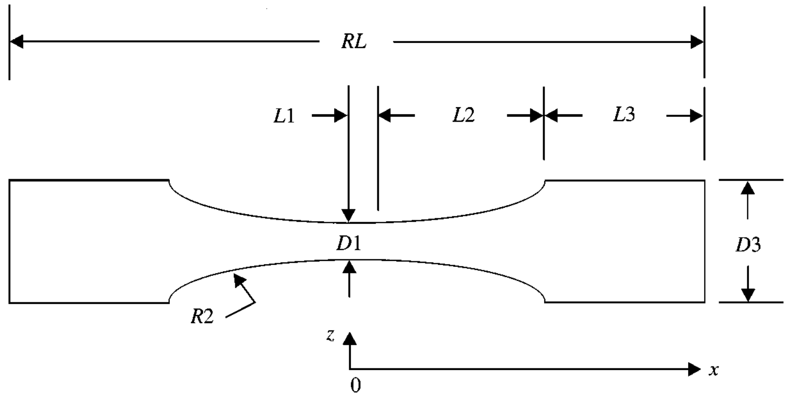

Figure 1. Longitudinal section of dog-bone-shaped specimen: $L1$, gage length; $D1$, gage diameter; $L2$, transition length; $R2$, radius of curvature; $L3$, end length, $D3$, end diameter; RL, resonance length. The center of the specimen corresponds to ($x = 0$, $z = 0$).

This equation was solved numerically using a fourth order Runge–Kutta method with Gill's modification [8]. The solution of equation (9) provided the stress and strain distribution along the length of the specimen, the resonance length for a given geometry of the dog-bone-shaped specimen and given frequency of ultrasonic excitation, as well as the magnification factors for various specimen geometries, as shown in Figure 1.

3. SPECIMEN GEOMETRY

Three different types of dog-bone-shaped specimens for ultrasonic fatigue testing are identified, with regard to their sections perpendicular to the longitudinal axis: (a) specimens with circular cross-section, (b) specimens with rectangular cross-section made from a thick plate, and (c) plate-like specimens made from a metallic sheet. Samples with circular cross-section are the ones most commonly used in ultrasonic fatigue [9]. However, plate-like specimens, often used in low cycle fatigue, may offer considerable advantages, such as the possibility of comparing the data from various testing configurations (high cycle and low cycle fatigue). Also, plate-like specimens are more convenient for performing *in situ* non-destructive inspection of the samples to monitor damage evolution, such as the onset of cracking and crack propagation.

3.1. CIRCULAR CROSS-SECTION DOG-BONE SPECIMENS MADE FROM A BAR

The cross-sectional area in this case is

$$A(x) = \pi z^2(x) \tag{11}$$

and $G(x)$, from equation (10) is written as

$$G(x) = \frac{2}{z(x)}\frac{\mathrm{d}z(x)}{\mathrm{d}x}. \tag{12}$$

3.2. RECTANGULAR CROSS-SECTION DOG-BONE SPECIMENS MADE FROM A THICK PLATE

There is a variable cross-section along both the thickness (y-axis) and the width (z-axis) of the sample. The cross-sectional area in this case is

$$A(x) = 4y(x)z(x) \tag{13}$$

and $G(x)$ is expressed as

$$G(x) = \frac{\mathrm{d}y(x)/\mathrm{d}x}{y(x)}\frac{\mathrm{d}z(x)/\mathrm{d}x}{z(x)}. \tag{14}$$

3.3. PLATE-LIKE SPECIMENS MADE FROM A METALLIC SHEET

For this type of specimens, the non-constant cross-section is only along the width (z-axis) of the sample, the thickness of the specimen being constant, y_0. The cross-sectional area in this case is

$$A(x) = 4z(x)y_0 \tag{15}$$

and $G(x)$ is given as

$$G(x) = \frac{1}{z(x)} \frac{\mathrm{d}z(x)}{\mathrm{d}x}. \tag{16}$$

Note that the general solution of differential equation (9) is the same for the above types of specimens. The difference in the $G(x)$ function between circular cross-section and plate-like specimen types is a factor of 2.

According to Figure 1 the following relationship is obtained:

$$z(x) = R1 + R2 - \sqrt{R2^2 - (x - L1)^2} \tag{17}$$

with $z(0) = z(L1) = D1/2 = R1$, $R2 = [L2^2 + (R3 - R1)^2]/2(R3 - R1)$, and $z(L1 + L2) = D3/2 = R3$. An analogous relationship can also be written for $y(x)$.

Next, let us study the example of a dog-bone-shaped specimen with circular cross-section with the geometry shown in Figure 1. The specimen is considered to be consisting of six homogeneous elements, each of the same elastic properties. It is assumed that the forces and the velocities are continuous across the interfaces. The specimen geometry is symmetric about the z-axis at $x = 0$. Based on these assumptions, the cross-sectional area of the specimen can be described as follows:

$$A(x) = \pi R1^2 \quad \text{when } 0 < x < L1,$$

$$A(x) = \pi R3^2 \quad \text{when } L1 + L2 < x < L3,$$

$$A(x) = \pi z^2(x) \quad \text{when } L1 < x < L2 \text{ (according to equation (11))}.$$

From equation (12),

$$G(x) = \frac{2\,R2 \sin\theta_x}{[(R1 + R2)/\sqrt{R2^2 - (x - L1)^2}] - 1}, \tag{18}$$

where, $\theta_x = a\tan(x - L1)/\sqrt{R2^2 - (x - L1)^2})$.

Based on the numerical calculations, plots of strain and displacement variations along the lengths of various specimens with different geometry are shown in Figure 2. The specimen geometry as well as the corresponding magnifications are specified in Table 1. As can be observed, the specimen is designed with an overall length equal to the resonance length so that the center of the specimen is the point of maximum strain. It should be noted that the maximum strain point is a nodal point for the displacement wave [10].

Figure 2(a) shows the distribution of strain and displacement along the length of a cylindrical specimen. As expected, the maximum strain is in the middle of the specimen, which corresponds to a node point for the displacement. The amplitude for the displacement is maximum at the two ends of the specimen. The maximum strain in the center of the specimen is obtained when the overall length of the sample is equal to the resonance length. As the overall length of the specimen deviates from the resonance length, the strain at the center of the specimen will decrease. It should be noted that the diameter of a cylindrical specimen has no effect on the strain produced.

Figures 2(b–d) show the distribution of strain and displacement along the length of dog-bone-shaped samples with different geometry. Based on this analysis, the fatigue specimen geometry can be modified to apply the desirable amount of strain on the samples.

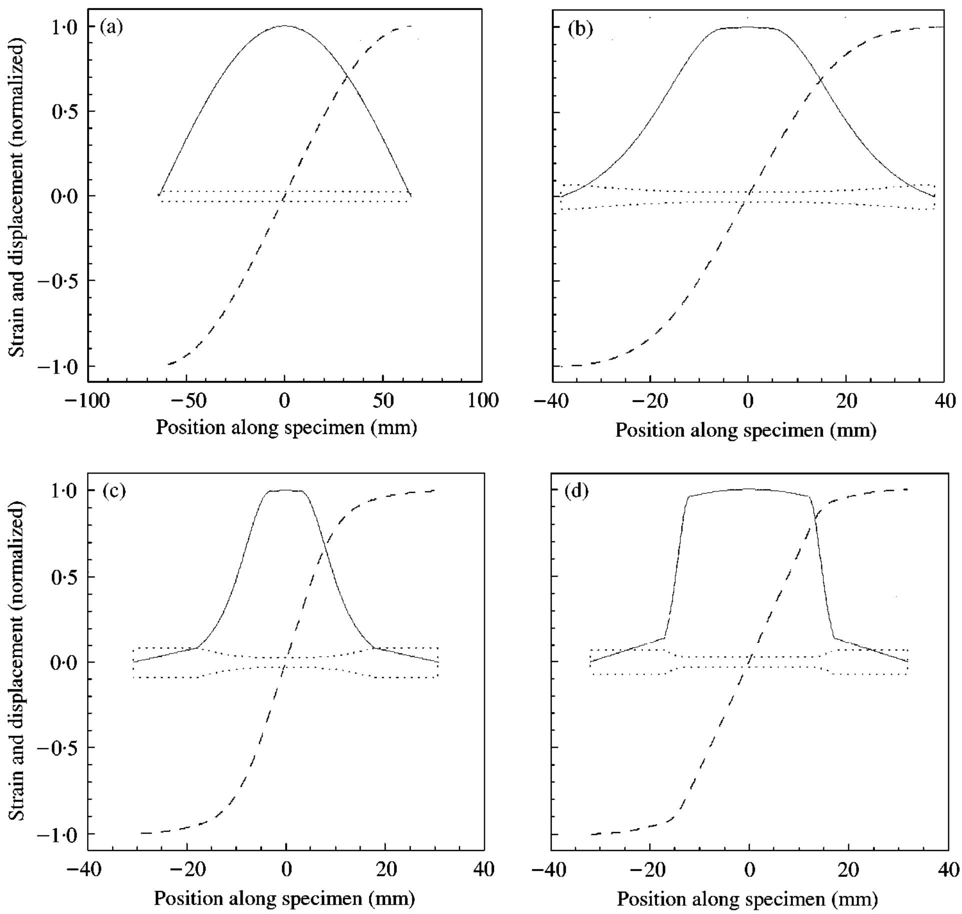

Figure 2. (a) Strain (——) and displacement (– – –) distribution for cylindrical Ti–6 Al–4V specimen. The specimen geometry is shown by (····) line; (b)–(d) strain (——) and displacement (– – –) distribution for dog–bone Ti–6 Al–4 V specimen (geometry shown in Table 1). The specimen geometry is shown by ···· line.

TABLE 1

Specimen geometry for Ti–6 Al–4 V samples (the dimensions are in mm)

Specimen	*D*1	*D*3	*L*1	*L*2	*L*3	*RL*	Magnification
Sample in Figure 2(a) (cylinder)	10	10	32	0	32	128	1
Sample in Figure 2(b)	4	10	5	30	3·15	76·3	2·06
Sample in Figure 2(c)	4	12	3	15	12·73	61·46	3·72
Sample in Figure 2(d)	4	10	12	5	14·9	63·8	2·59

4. INFLUENCE OF MATERIAL PROPERTIES AND ULTRASONIC FREQUENCY ON THE SAMPLE RESONANCE LENGTH

Figure 3 shows the maximum strain (at the center of the specimen) and the resonance length as a function of E/ρ. Results for different materials are shown in this figure and are summarized in Table 2. It is suggested that specimens with lower ultrasonic velocity,

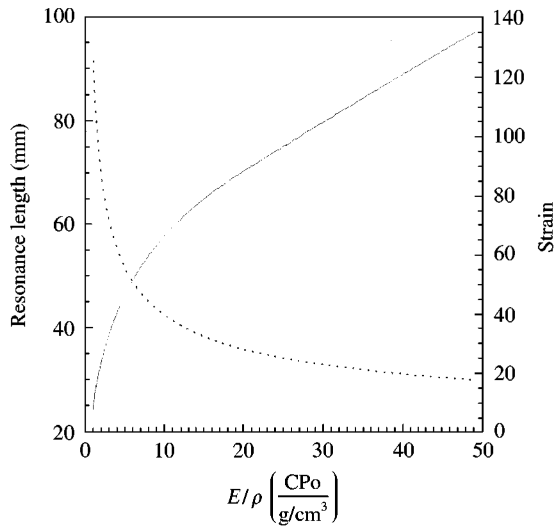

Figure 3. Maximum strain (·····) and resonance length (——) as a function of material properties.

TABLE 2

Material characteristics and ultrasonic response

Material	E (GPa)	ρ (g/cm^3)	c (m/s)	E/ρ	RL (mm)	Magnification
Ti–6 Al–4V	116	4·43	5117	26·2	76·3	2·06
Nickel	119	8·9	4729	22·4	72·6	1·94
Copper	129	8·92	3803	14·5	64·3	1·67
Lead	16	11·34	1188	1·4	28·3	2·83
Magnesium	45	1·74	5085	25·9	76	2·05
Brass	92	8·47	3296	10·9	59·2	1·53
Steel	200	7·8	5064	25·6	75·8	2·05
Al 2024-T3	70·3	2·77	5038	25·4	75·7	2·04

$c = \sqrt{E/\rho}$, will undergo higher strains for a given power level and will require a smaller overall length. Note that the magnification (given in Table 2 for various materials) is not a monotonic function of E/ρ.

The plot in Figure 4 shows the overall length of a specimen (resonance length) as a function of ultrasonic frequency for a given shape of the specimen. The relationship is nonlinear. It can be observed that for low ultrasonic frequencies (below 15 kHz) the resonance length of the specimen becomes very large (95 mm for 15 kHz, 346 mm for 5 kHz, etc.). Also, the magnification increases as the frequency decreases. Above 15 kHz the resonance length decreases at a slower rate compared to low frequencies. For example, at 20 kHz the resonance length is 76·3 mm with a magnification of 2·06, at 30 kHz the resonance length is 60·4 mm with a magnification of 1·56, and at 40 kHz the resonance length is 50·55 mm with a magnification of 1·33.

Figure 5 shows the amplification of the displacement wave as a function of diameter at the center of a specimen (normalized by the diameter at the specimen end). This plot illustrates the concept that selecting appropriate specimen geometry can modify the

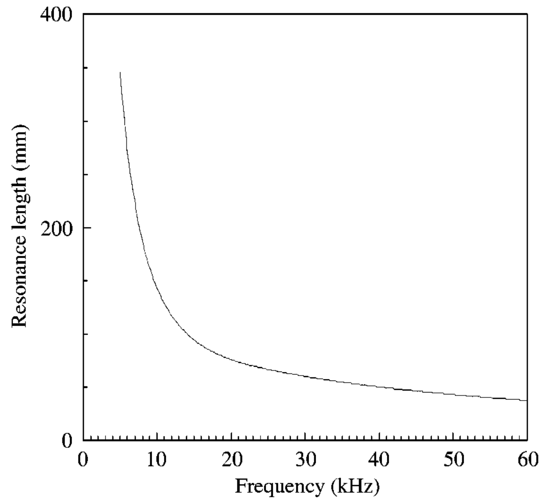

Figure 4. Dependence of sample resonance length on ultrasonic frequency for Ti–6 Al-4V.

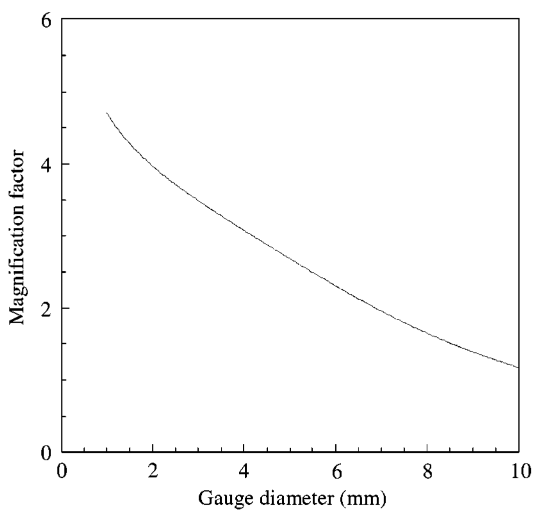

Figure 5. Magnification versus diameter at the center of the specimen (gage diameter).

amplification. The lower limit for the magnification factor is 1, when the gage diameter becomes equal to the diameter at the ends of the specimen (case of a cylindrical sample).

5. SUMMARY

An analysis was carried out to calculate the resonance length, strain and displacement along the length of fatigue specimens with different geometries and for various resonant frequencies. The theoretical calculations help in optimizing the design of fatigue samples for testing at ultrasonic frequencies. Results for a variety of types of specimen that may be used in ultrasonic fatigue are presented. These types of specimen include circular cross-section dog-bone specimens made from a bar, rectangular cross-section dog-bone specimens made from a thick plate, and plate-like specimens made from a metallic sheet. Several findings of the analysis are summarized below.

The strain is maximum at the center and null at the two ends of the specimen. Contrarily, the displacement is maximum at the two ends and null at the center of the specimen. The strain at the center of the specimen decreases as the overall length of the specimen deviates from the resonance length. The material property plays an important role in the resonance length. Specimens with lower ultrasonic velocity will be subjected to higher strains for a given power level and therefore require a smaller resonance length. The resonance length is a non-linear function of ultrasonic frequency for a given shape of the specimen and the magnification increases as the frequency decreases. Selecting appropriate specimen geometry can modify the amplification of ultrasonic stresses induced in the material.

ACKNOWLEDGMENTS

This work was sponsored by the Defense Advanced Projects Agency (DARPA) Multidisciplinary University Research Initiative (MURI), under Air Force Office of Scientific Research grant number F49620-96-1-0442.

REFERENCES

1. W. P. MASON 1950 *Piezoelectric Crystals and Their Application in Ultrasonics*, 161. New York: Van Nostrand.
2. E. A. NEPPIRAS 1959 *Proceedings of the American Society for Testing Materials* **59**, 691–709. Techniques and equipment for fatigue testing at very high frequencies.
3. E. EISNER and J. S. SEAGER 1963 *Report No.* 216, *H. M. Stationary Office*, *London*. Safety in mines research establishment.
4. E. EISNER 1964 *Journal of the Acoustical Society of America* **36**, 309.
5. W. P. MASON and R. F. WICK 1951 *Journal of the Acoustical Society of America* **23**, 209.
6. W. HOFFELNER 1982 645–657. Fatigue of high temperature materials at ultrasonic frequencies.
7. T. E. MATIKAS 2001 *Fatigue and Fracture of Engineering Materials & Structures*, submitted. A high cycle fatigue apparatus at 20 kHz for LCF/HCF interaction testing.
8. T. E. SHOUP 1984 *Applied Numerical Methods for the Microcomputer*, 116–123, Englewood Cliffs, NJ: Prentice-Hall.
9. 1999 *Fatigue and Fracture of Engineering Materials and Structures*, *Special Issue* **22**.
10. J. DROSSIS 1991 *Master's Thesis*, *University of Toronto*. The design development and commissioning of a test facility for HCF/LCF interactive tests.